JOURNAL OF SOLID STATE CHEMISTRY 59, 324–331 (1985)

The Phase Study of the Tl–V–S System and the Properties of TlV_6S_8 and TlV_5S_8 Phases

T. OHTANI AND S. ONOUE

Okayama University of Science, Laboratory for Solid State Chemistry, 1-1 Ridai-cho, Okayama 700, Japan

Received December 10, 1984; in revised form March 22, 1985

The ternary phase diagram of the Tl–V–S system was investigated using samples quenched from 400°C, especially in the neighborhood of TlV_6S_8 and TlV_5S_8 phases. The TlV_6S_8 phase ($Tl_xV_6S_y$) exists between $0.75 < x < 1.00$ and $7.55 < y < 7.90$, and the TlV_5S_8 phase ($Tl_{x'}V_5S_{y'}$) between $0.70 < x' < 1.00$ and $7.54 < y' < 7.98$. A new ternary phase with the nominal composition of TlV_2S_4 was found in addition to the three known ternary phases. The entirely deintercalated $V_6S_{7.8}$ with the framework structure was obtained by using 1 *N* $AlCl_3$ + 0.01 *N* $FeCl_3$ aqueous solution, while the lower phase limit of the TlV_5S_8 phase was $Tl_{0.33}V_5S_8$ consistent with the earlier work. The electrical resistivity and the magnetic susceptibility measurements show that these compounds are expected to be weakly magnetic itinerant-electron systems.

Introduction

The ternary compounds TlV_6S_8 and TlV_5S_8 were first prepared by Vlasse and Fournès *et al.* (*1–4*). TlV_6S_8 has a hexagonal structure (space group $P6_3$) isostructural with the Nb_3Te_4-type structure which is constructed with VS_6 octahedra sharing common faces and edges, forming the Tl containing hexagonal channels parallel to the *c* axis (*1*) (Fig. 1a). TlV_5S_8 has a monoclinic symmetry with space group $C2$ (*2*). This structure also is made up of VS_6 octahedra joining common faces and edges with the large rectangular channels along the b axis into which are inserted the thallium atoms (Fig. 1b).

TlV_6S_8 and TlV_5S_8 have the following common characteristics. (1) Both can be described as channel compounds. The guest cations in the lattice channels can be easily intercalated and deintercalated (*5–8*). (2) Both have isolated vanadium–vanadium zigzag chains running parallel to the crystalline axis (along the *c* axis in TlV_6S_8, and the *b* axis in TlV_5S_8), which are responsible for the high metallic and anisotropic conductivity (*1, 2*).

There are some problems which remain unsolved. No metallurgical study has yet been done on these compounds, and thus little is known about their stability ranges so far. In addition, there is no report on the preparation of the entirely deintercalated V_6S_8 or V_5S_8 with the framework structure, although it is of importance from the crystallochemical point of view to obtain these binary compounds which are not stable at equilibrium. Fournès and Vlasse reported that TlV_6S_8 and TlV_5S_8 are both Pauli paramagnetic metals (*1–4*). However, resistivity measurements have not yet been per-

0022-4596/85 $3.00

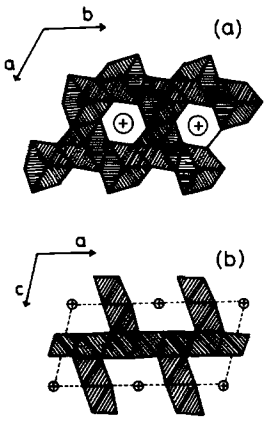

FIG. 1. Structures of TlV_6S_8 (a) and TlV_5S_8 (b); circles indicate the positions of thallium atoms (Refs. (*1*, *2*, *7*)).

formed in the low-temperature region below 80 K.

The present investigation consists of three parts. First, we performed the phase study of the ternary Tl–V–S system especially in the vicinity of TlV_6S_8 and TlV_5S_8, and clarified the stability ranges of these two compounds along with the phase relationships among their neighboring phases. Second, we prepared the new binary compound, V_6S_8, with the framework structure of TlV_6S_8 by means of the deintercalation method. Third, we measured the temperature dependence of the magnetic susceptibility (χ) and the electrical resistivity (ρ) of these compounds.

Experimental

Samples of the Tl–V–S system were synthesized directly from the elements. Starting materials were treated in a drybox under purified argon atmosphere. The vacuum-sealed components in silica tubes were slowly heated up to 1000°C during 12 days, kept at this temperature for 2 days, and subsequently cooled down to room temperature for 12 days. Samples thus obtained were annealed at the desired temperatures, followed by quenching into water. The phase analysis was carried out mainly by the powder X-ray diffraction method using Cu$K\alpha$ radiation. Chemical compositions of some representative compounds were checked by both X-ray microanalysis and chemical analysis. The chemical analysis was carried out in the following manners. Sulfur was analyzed by the wet method by burning samples under oxygen atmosphere, and absorbing the produced SO_2 gas into H_2O_2 aqueous solution. Thallium was analyzed by converting the samples to TlI by using KI solution. Vanadium content was estimated from the sulfur and the thallium contents. In the case of the deintercalated V_6S_8, the vanadium was analyzed directly by oxidizing the samples in the air. Density measurements were carried out by immersion method, using toluene.

The deintercalation of thallium in TlV_6S_8 and TlV_5S_8 was accomplished with iodine solution in acetonitrile or with 1 *N* $AlCl_3$ aqueous solution. In the latter case, the deintercalation was carried out at the boiling temperature of the solution in order to accelerate the reaction. At the final stage of reaction, the aqueous solution, 1 *N* $AlCl_3$ + 0.01 *N* $FeCl_3$ was used. Obtained deintercalated samples were heated at 200°C under vacuum in order to evaporate the free sulfur which was produced during the reaction although the quantity was very small.

The possibility of oxygen uptake into the lattice was excluded by the results of the X-ray microanalysis and the chemical analysis. This possibility was also excluded by the magnetic susceptibility measurements, because there was no indication of the phase transition which could be observed in the vanadium oxides.

Electrical resistivity measurements were carried out by a dc four-probe method on powdered pressed pellets from 2 to 280 K. Magnetic susceptibility measurements were performed by a Faraday-type torsion

balance and a pendulum magnetometer from 4.2 to 290 K.

Results and Discussion

1. Phase Relations

Phase equilibria of the Tl–V–S system in the vicinity of TlV_6S_8 and TlV_5S_8 were investigated experimentally at 400°C, and were summarized in an isothermal diagram (Fig. 2). Selected representative data used to define the assemblages are given in Table I. On the V–S join, we observed the following known binary phases: V_4S_4(tetragonal, Ti_5Te_4-type), VS(hexagonal, NiAs-type), V_3S_4(monoclinic, Cr_3S_4-type), and V_5S_8 (monoclinic, V_5S_8-type). These results are consistent with previous work on the binary V–S system (*9, 10*). On the Tl–S join, we observed only Tl_2S(hexagonal, anti-CdI_2-type). This compound does not show an appreciable nonstoichiometric range. We did not find another known phase, TlS, because of its low melting temperature (274°C). The ternary phases whose existences are so far confirmed are Tl_3VS_4 (*11*), TlV_6S_8, and TlV_5S_8 (*1–4*). The present study revealed their homogeneity ranges. Tl_3VS_4 has a relative wide stability range which spreads toward less-thallium and more-vanadium composition from the stoichiometry. DTA measurements of this compound showed the melting point at 500°C. TlV_6S_8 as well as TlV_5S_8 phase has the rather wide variation in thallium content x, compared to the ratio V/S.

In the present investigation, we found the new phase with the nominal composition of TlV_2S_{4+x} ($0 < x < 0.5$). For convenience,

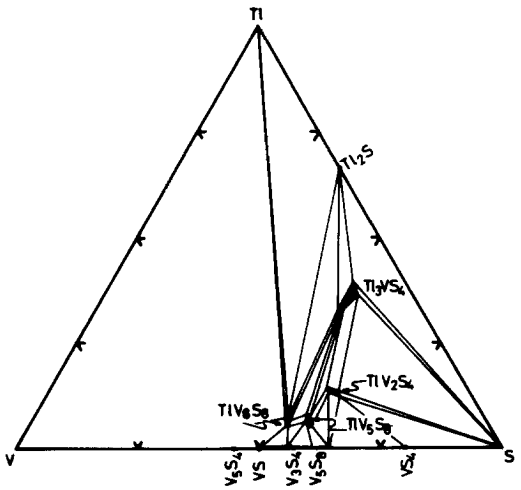

FIG. 2. Partial ternary Tl–V–S phase diagram at 400°C as determined from the study of quenched samples.

TABLE I

SAMPLES COMPOSITIONS AND X-RAY IDENTIFICATION OF PHASES PRESENT FOR THE SAMPLES QUENCHED FROM 400°C

Run No.	Bulk composition (at.%) Tl	V	S	Phase detected at room temperature
284	8.2	40.8	51.0	TlV_6S_8 + VS + Tl
091	8.0	40.0	52.0	TlV_6S_8 + Tl
289	8.0	39.9	52.1	TlV_6S_8 + Tl_2S
245	6.7	40.3	53.0	TlV_6S_8 + Tl_3VS_4
294	7.8	39.2	53.0	TlV_6S_8 + TlV_5S_8 + Tl_3VS_4
321	6.3	41.5	52.2	TlV_6S_8 + VS
244	6.8	40.5	52.7	TlV_6S_8
324	6.1	40.7	53.2	TlV_6S_8 + TlV_5S_8
328	3.6	43.2	53.2	TlV_6S_8 + V_3S_4
339	0.4	43.6	56.0	V_3S_4
337	2.1	42.9	55.0	TlV_6S_8 + TlV_5S_8 + V_3S_4
312	0.7	42.4	57.9	TlV_5S_8 + V_3S_4
257	0.1	38.4	61.5	V_5S_8
258	0.4	38.3	61.3	TlV_5S_8 + V_5S_8
279	8.3	35.7	56.0	TlV_5S_8 + Tl_3VS_4
260	6.6	35.9	57.5	TlV_5S_8 + TlV_2S_4
214	10.0	33.3	56.7	TlV_5S_8 + TlV_2S_4 + Tl_3VS_4
206	5.9	32.2	61.9	TlV_5S_8 + TlV_2S_4 + V_5S_8
145	37.5	12.5	50.0	Tl_3VS_4
524	14.0	27.9	58.1	TlV_2S_4
533	7.5	30.0	62.5	TlV_2S_4 + V_5S_8
527	13.0	26.1	60.9	TlV_2S_4 + S
536	7.0	27.9	65.1	TlV_2S_4 + V_5S_8 + S
457	22.2	22.2	55.6	TlV_2S_4 + Tl_3VS_4
453	16.0	24.0	60.0	TlV_2S_4 + Tl_3VS_4 + S
375	38.7	13.3	48.0	Tl_3VS_4 + Tl_2S
372	40.0	10.0	50.0	Tl_3VS_4 + Tl_2S + S
528	9.8	29.2	61.0	TlV_2S_4 + V_5S_8

we designate this phase as the TlV_2S_4 phase. This phase has the dark-purple color and sometimes tiny thin crystals were grown in the reaction tubes. The powder X-ray diffraction pattern of this phase was indexed hexagonal. The lattice parameters of $TlV_2S_{4.17}$ were $a = 3.219$ Å and $c = 8.10 \times 2$ Å, which are well consistent with the results of density measurements (d_{obs} = 5.00 g cm^{-3}). DTA studies on this phase showed the reversible phase transition to the other new phase with hexagonal symmetry at 520°C. The lattice parameters of the high-temperature phase were $a = 3.296$ Å and $c = 8.02 \times 2$ Å. This phase showed the decomposition into TlV_5S_8, Tl_3VS_4, and Tl_2S at 760°C. These new phases seem to be the intercalation compounds such as $Tl_{0.5}TaS_2$ (*12*). Using single crystals we are in the progress of determining the structure of these phases and details will be published elsewhere.

Fournès and Vlasse have reported the other new phase, $Tl_2V_2S_5$, which has orthorhombic symmetry with the space group $C222_1$ (*3, 4*). In the present investigation, we could not find it at the corresponding composition above 450°C. This phase would be stable at the lower temperatures. However, the curious fact is that the X-ray pattern of the present new phase TlV_2S_{4+x} ($x > 0.33$) is very similar to that $Tl_2V_2S_5$ phase. These problems remain for the future work.

The enlarged portions of the phase fields of TlV_6S_8 and TlV_5S_8 are shown in Fig. 3. For the graphic presentation of the single-phase regions, we chose the perfect V sublattices ($Tl_xV_6S_y$ and $Tl_{x'}V_5S_{y'}$); this is similar to the method adopted for the Chevrel compound $Pb_xMo_6S_{8-y}$ (*13*). This presentation is quite reasonable in the present case because our density measurements revealed that both TlV_6S_8 and TlV_5S_8 phases have the sulfur vacancies, not the vanadium interstitials. The results of density measurements for TlV_6S_8 phase are as follows; the observed density of $V_6S_{7.8}$ with the framework structure (preparation of this compound will be described below) is $d_{obs}(V_6S_{7.8}) = 3.86$ g cm^{-3}, which is consistent with the theoretical density with the assumption that the compound contains only the sulfur vacancies, $d_{theor}(V_6S_{8-0.2}) = 3.862 \pm 0.002$ g cm^{-3}, while the theoretical density with the assumption of the presence of the vanadium interstitials only is $d_{theor}(V_{6+0.15}S_8) = 3.961 \pm 0.002$ g cm^{-3}. The results for TlV_5S_8 phase are as follows; the observed density of $Tl_{1.0}V_5S_{7.8}$ is $d_{obs}(Tl_{1.0}V_5S_{7.8}) = 4.93$ g cm^{-3} and the theoretical density with the assumption of the presence of sulfur vacancies only is $d_{theor}(Tl_{1.0}V_5S_{8-0.2}) = 4.928 \pm 0.004$ g cm^{-3}.

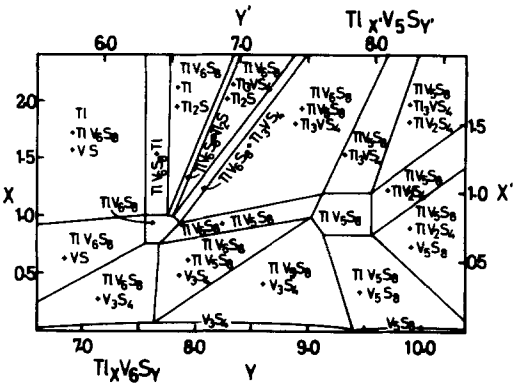

FIG. 3. Phase fields of TlV_6S_8 and TlV_5S_8 phases as determined from the samples quenched from 400°C. The compositions of $Tl_xV_6S_y$ and $Tl_{x'}V_5S_{y'}$ are indicated by the left-hand-side ordinate and the lower abscissa, and by the right-hand-side ordinate and the upper abscissa, respectively.

The single-phase region of $Tl_xV_6S_y$ exists between $0.75 < x < 1.00$ and $7.55 < y < 7.90$ (errors are $|\Delta x| \leqq 0.01$ and $|\Delta y| \leqq 0.025$). One of the notable results is that the TlV_6S_8 phase is not stable at the stoichiometric composition; the S/V ratio is as much as 7.8/6.0, which implies this phase is stabilized by the formation of sulfur vacancies. Another feature worth mentioning is that the stability range of this phase is restricted in the rather high thallium content,

in contrast with the results of Vlasse and Fournès ($0.50 < x < 0.85$) (*3*) and with that of Eckert *et al.* ($x \leqq 0.61$) (*7*). In the thallium-rich portion of the system, TlV_6S_8 phase coexists with Tl, Tl_2S, and Tl_3VS_4 phases; from the left- to the right-hand side in this region, the following two- or three-phase regions appear; TlV_6S_8 + Tl, TlV_6S_8 + Tl + Tl_2S, TlV_6S_8 + Tl_2S, TlV_6S_8 + Tl_3VS_4 + Tl_2S, and TlV_6S_8 + Tl_3VS_4. On the low-thallium side there are: two-phase region TlV_6S_8 + V_3S_4, three-phase region TlV_6S_8 + TlV_5S_8 + V_3S_4, and the single-phase region V_3S_4. The TlV_6S_8 phase coexists with VS on the sulfur-poor side and with TlV_5S_8 on the sulfur-rich side.

TABLE II

THE X-RAY DIFFRACTION PATTERN OF THE DEINTERCALATED $V_6S_{7.8}$

hkl	d_{obs}(A)	d_{calc}(A)	I_{obs}	I_{calc}
100	7.971	7.912	vs	100
110	4.594	4.568	vw	3
200	3.965	3.956	vw	2
101	3.054	3.049	w	15
210	2.994	2.990	w	8
300	2.639	2.637	w	8
201	2.540	2.536	w	14
220	2.284	2.284	vw	3
211	2.218	2.217	s	54
310	2.195	2.194	m	24
301	2.060	2.061	vw	4
400	1.977	1.978	vw	3
221	1.879	1.879	m	30
410	1.726	1.727	w	8
002	1.653	1.652	w	10
321	1.590	1.591	w	20
500	1.581	1.582	vw	4
411	1.529	1.530	vw	2
420	1.495	1.495	vw	3
510	1.422	1.421	vw	4
331	1.382	1.383	vw	1
421	1.361	1.362	vw	4
312	1.320	1.320	w	7
600		1.319		2
511	1.305	1.305	vw	2
520	1.268	1.267	vw	1
610	1.207	1.207	vw	2

Note. Calculation is based on the TlV_6S_8-type structure with the space group $P6_3$.

The TlV_5S_8 phase has nearly the same size of homogeneous area as the TlV_6S_8 phase. The stability range of this phase lies between $0.70 < x' < 1.00$ and $7.54 < y' < 7.98$ for $Tl_{x'}V_5S_{y'}$ (errors are $|\Delta x'| \leqq 0.05$ and $|\Delta y'| \leqq 0.01$). This phase also is not stable at the stoichiometric composition. The single-phase region spreads toward the less-sulfur side from the stoichiometry. On the thallium-rich side, the TlV_5S_8 phase coexists with TlV_6S_8, Tl_3VS_4 and TlV_2S_4 phases; the following two- or three-phase regions appear in this region: TlV_6S_8 + TlV_5S_8 + Tl_3VS_4, TlV_5S_8 + Tl_3VS_4, and TlV_5S_8 + TlV_2S_4 + Tl_3VS_4. In the low thallium portion, there exist the following regions: TlV_6S_8 + TlV_5S_8 + V_3S_4, TlV_5S_8 + V_3S_4, TlV_5S_8 + V_5S_8, and TlV_5S_8 + TlV_2S_4 + V_5S_8. No three-phase region with any significant width could be detected between the above two-phase region, which may be related to the absence of a two-phase region between V_3S_4 and V_5S_8 (*9, 10*). The TlV_5S_8 phase coexists with the TlV_6S_8 phase at the low-sulfur side, and with the TlV_2S_4 phase at the sulfur-rich side.

The phase boundaries of both TlV_6S_8 and TlV_5S_8 phases were scarcely affected by quenching temperatures up to 1000°C.

2. *Deintercalation*

2.1. TlV_6S_8 phase. Schöllhorn removed the thallium ions from $Tl_{0.6}V_6S_8$ by the topotactic anodic oxidation process, and obtained the metastable phase with the thallium content ranging down to $x = 0.17$ (*7*). In the present investigation, we could prepare the entirely deintercalated $V_6S_{7.8}$ by using the $AlCl_3$ + $FeCl_3$ aqueous solution as described before. $V_6S_{7.8}$ thus obtained is very stable in the air, and shows a sharp X-ray pattern. In Table II, the powder X-ray pattern of $V_6S_{7.8}$ is compared with the calculation based on the TlV_6S_8-type structure with the space group $P6_3$. The good coinci-

dence between the observation and the calculation indicates the V–S framework remains unchanged during the deintercalation process. Figure 4 shows the variation of lattice parameters with the thallium concentration for $Tl_xV_6S_{7.8}$ system. The lattice constant a decreases continuously with decreasing thallium content, while c slightly increases with decreasing thallium content. The contraction of the unit cell volume is 1.3%. DTA measurements of $V_6S_{7.8}$ showed a broad exothermic irreversible transition at around 700°C. The X-ray diffraction pattern of samples quenched from above the transition temperature was identical with that of V_3S_4 with the Cr_3S_4-type structure.

2.2. TlV_5S_8 phase. Schöllhorn *et al.* obtained the nonstoichiometric $Tl_xV_5S_8$ with the lower phase limit of $Tl_{1/3}V_5S_8$ either by galvanostatic oxidation or by chemical oxidation with 1 *M* aqueous $FeCl_3$ solution (*6, 8*). From the ^{205}Tl and ^{51}V NMR data, they observed a unique behavior in this compound; in the course of oxidation the charge of the host lattice remains constant, while the charge of Tl ions is changed from Tl^{1+} in $Tl^{1+}(V_5S_8)^{-1}$ to Tl^{3+} in $(Tl^{3+})_{1/3}(V_5S_8)^{1-}$. The lower limit of the thallium content in the present work is consistent with their results. Figure 5 shows the thallium concentration dependence of lattice parameters of $Tl_xV_5S_{7.8}$. The lattice constants a, b, and c continuously decrease with decreasing thallium content in the range of $0.33 \leqq x \leqq 1.0$, while the angle β is nearly constant with x. The ratios c/a and c/b also are scarcely variable with x. These results imply that the $Tl_xV_5S_8$ lattice contracts without distortion during the deintercalation. The continued deintercalation beyond $x = 0.33$ lead to the appearance of the additional phase of V_5S_8.

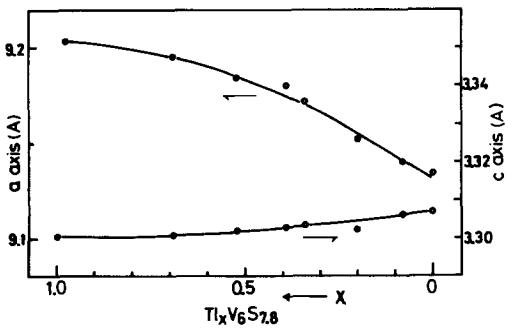

FIG. 4. The x dependence of lattice parameters for the deintercalated $Tl_xV_6S_{7.8}$.

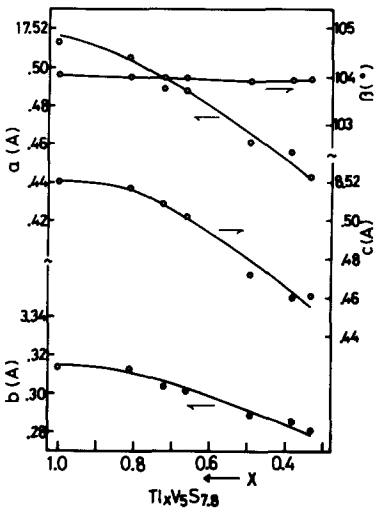

FIG. 5. The x dependence of lattice parameters for the deintercalated $Tl_xV_5S_{7.8}$.

3. Electrical and Magnetic Properties

The observed temperature dependence of the relative resistivity $\rho'(\rho(T)/\rho(280\ K))$ of $Tl_{1.0}V_6S_{7.8}$ and $Tl_{1.0}V_5S_{7.8}$ is shown in Fig. 6. In both compounds the resistivity shows the metallic behavior without any anomaly in the measured temperature range from 2 to 280 K. It should be noted that the ρ'–T curve of both compounds is not of the normal metallic behavior; i.e., ρ' gradually increases with temperature at the low-temperature region, and then sharply increases up to about 100 K, followed by the tendency of saturation in the high-temperature region. This temperature dependence of ρ' is quite similar to that reported by Bronsema *et al.* for $K_{0.5}V_5S_8$ which is isostructural with TlV_5S_8 (*14*).

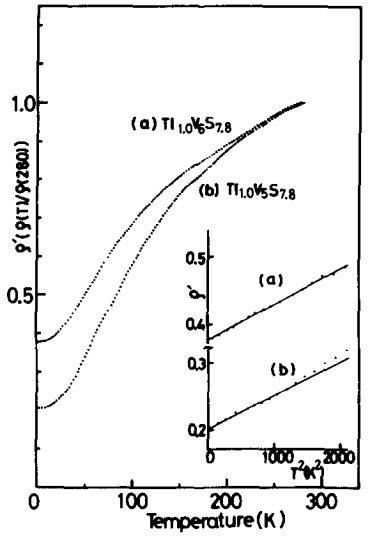

FIG. 6. Temperature dependence of the relative electrical resistivity $\rho'(\rho(T)/\rho(280\ \text{K}))$ of powered pressed pellets of $Tl_{1.0}V_6S_{7.8}$ and $Tl_{1.0}V_5S_{7.8}$. The inset gives a T^2 dependence of the relative electrical resistivity.

The inset gives the T^2 dependence of ρ' for both compounds; ρ' is proportional to T^2 below about 45 K and below about 35 K for $Tl_{1.0}V_6S_{7.8}$ and $Tl_{1.0}V_5S_{7.8}$, respectively. It is well known that T^2 dependence of ρ at low temperatures is observed in metallic compounds with highly correlated electron systems (*15*). In the present case, we can roughly estimate the coefficient of the T^2 term (we designate this term as A) to be 1.33×10^{-1} and 5.2×10^{-2} $\mu\ \Omega$ cm K^{-2} for $Tl_{1.0}V_6S_{7.8}$ and $Tl_{1.0}V_5S_{7.8}$, respectively. These values are of the same order as those of the well-known itinerant magnetic compounds such as $ZrZn_2$ (*16*), Sc_3In (*17*), V_2O_3 (*18, 19*) (for these compounds $A \sim 5 \times 10^{-2}$ $\mu\ \Omega$ cm K^{-2}).

In Fig. 7 are given the temperature dependence of the magnetic susceptibility (χ) of $Tl_xV_6S_{7.8}$ ($x = 0$, 1.0) and $Tl_{1.0}V_5S_{7.8}$. $Tl_{1.0}V_6S_{7.8}$ shows the temperature-independent Pauli paramagnetic behavior, consistent with the results of Vlasse and Fournès (*1*). The Curie–Weiss-like dependence at low temperatures may be due to the presence of magnetic impurities. Measurements in the high-temperature range up to 500 K did not show any anomaly except the slight increase with temperature. The $V_6S_{7.8}$ also shows a Pauli paramagnetic behavior essentially similar to $Tl_{1.0}V_6S_{7.8}$. The temperature dependence of χ of $Tl_{1.0}V_5S_{7.8}$ can be fitted to the Curie–Weiss law

$$\chi = \chi_0 + \frac{C}{T - \theta},$$

where χ_0, C, and θ are a temperature-independent term, a Curie constant, and a Weiss constant, respectively. Obtained magnetic parameters are as follows: $\chi_0 = 1.40 \times 10^{-3}$ emu/mole (1.97×10^{-6} emu/g), $C = 9.48 \times 10^{-2}$ emu · K/mole (1.34×10^{-4} emu · K/g), $P_{\text{eff}} = 0.39\ \mu_B$/mag · atom, and $\theta = -32$ K. The high value of χ_0 may suggest the presence of strong electron correlation effects in this compound.

As a result, the present measurements of ρ and χ suggest that $Tl_xV_6S_{7.8}$ and $Tl_xV_5S_{7.8}$ are the itinerant magnetic metals.

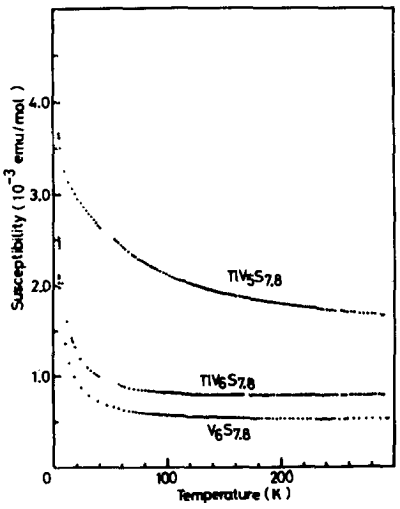

FIG. 7. Temperature dependence of the magnetic susceptibility of $Tl_xV_6S_{7.8}$ ($x = 0$, 1.0) and $Tl_{1.0}V_5S_{7.8}$.

Acknowledgments

The authors would like to thank Dr. H. Nishihara and Professor H. Yasuoka for fruitful discussions and suggestions and for offering a chance to carry out the magnetic susceptibility and the electrical resistivity measurements. It is also a pleasure to thank Professor M. Shibata and Mr. A. Nishi for performing the X-ray microanalysis. This work was supported in part by the Grant-in-Aid for Scientific Research from the Ministry of Education.

References

1. M. VLASSE AND L. FOURNÈS, *Mater. Res. Bull.* **11,** 1527 (1976).
2. L. FOURNÈS, M. VLASSE, AND M. SAUX, *Mater. Res. Bull.* **12,** 1 (1977).
3. L. FOURNÈS AND M. VLASSE, *Rev. Chim. Miner.* **15,** 542 (1978).
4. L. FOURNÈS, Doctoral thesis No. 580. University Bordeaux I (1978).
5. R. SCHÖLLHORN, *Angew. Chem. Int. Ed. Engl.* **19,** 983 (1980).
6. W. SCHRAMM, R. SCHÖLLHORN, H. ECKERT, AND W. MÜLLER-WARMUTH, *Mater. Res. Bull.* **18,** 1283 (1983).
7. H. ECKERT, W. MÜLLER-WARMUTH, W. SCHRAMM, AND R. SCHÖLLHORN, *Solid State Ionics* **13,** 1 (1984).
8. R. SCHÖLLHORN, *in* "Physics of Intercalation Compounds" (L. Pietronero and E. Tosatti, Eds.), p. 33, Springer-Verlag, Berlin/New York (1983).
9. Y. OKA, K. KOSUGE, AND S. KACHI, *J. Solid State Chem.* **23,** 11 (1978); **24,** 41 (1978).
10. M. NAKANO-ONODA AND M. NAKAHIRA, *J. Solid State Chem.* **30,** 283 (1979).
11. C. CREVECOEUR, *Acta Crystallogr.* **17,** 757 (1964).
12. G. V. SUBBA RAO, M. W. SHAFER, AND J. C. TSANG, *J. Phys. Chem.* **79,** 553 (1975).
13. J. HAUCK, *Mater. Res. Bull.* **12,** 1015 (1977).
14. K. D. BRONSEMA, R. JANSEN, AND G. A. WIEGERS, *Mater. Res. Bull.* **19,** 555 (1984).
15. T. MORIYA, *J. Magn. Magn. Mater.* **14,** 1 (1976).
16. S. OGAWA, *J. Phys. Soc. Jpn.* **40,** 1007 (1976).
17. T. HIOKI AND Y. MASUDA, *J. Phys. Soc. Jpn.* **43,** 1200 (1977).
18. D. B. MCWHAN, A. MENTH, J. P. REMEIKA, W. F. BRINCKMAN, AND T. M. RICE, *Phys. Rev. B* **7,** 1920 (1973).
19. N. F. MOTT, "Metal-Insulator Transition," Taylor & Francis, London (1974).